Mechanical and Aerospace Engineering Faculty Research & Creative Works

Mechanical and Aerospace Engineering

Dynamic Adiabatic Shear Band Development In A Bimetallic Body Containing A Void

R. C. Batra
Missouri University of Science and Technology

Z. G. Zhu

Recommended Citation

R. C. Batra and Z. G. Zhu, "Dynamic Adiabatic Shear Band Development In A Bimetallic Body Containing A Void," *International Journal of Solids and Structures*, vol. 27, no. 14, pp. 1829 - 1854, Elsevier, Jan 1991.
The definitive version is available at https://doi.org/10.1016/0020-7683(91)90015-8

DYNAMIC ADIABATIC SHEAR BAND DEVELOPMENT IN A BIMETALLIC BODY CONTAINING A VOID

R. C. BATRA and Z. G. ZHU

Department of Mechanical and Aerospace Engineering and Engineering Mechanics,
University of Missouri-Rolla, Rolla, MO 65401–0249, U.S.A.

Abstract—We study the problem of the initiation and subsequent growth of a shear band in a thermally softening viscoplastic prismatic body of square cross-section and containing two symmetrically placed thin layers of a different viscoplastic material and an elliptical void at the center. The yield stress of the material of the thin layer in a quasistatic simple compression test is taken to be either five times or one-fifth that of the matrix material. The body is deformed in plane strain compression at a nominal strain rate of 5,000 s^{-1}. These deformations are assumed to be symmetrical about the centroidal axes.

It is found that shear bands initiate from the ends of the major axes of the ellipsoidal void and propagate in the direction of the maximum shear stress. These bands are arrested by the strong virtually rigid material of the thin layer, but pass through the weaker material of the thin layer rather easily. Other shear bands originate from points where the thin layers meet the free boundaries and propagate into the matrix material along the direction of maximum shearing when the material of the thin layer is stronger, but propagate into the thin layer when its material is weaker than the matrix material. The band in the weaker material of the thin layer bifurcates into two bands that propagate into the matrix material in the direction of the maximum shearing stress.

1. INTRODUCTION

According to a recent paper of Johnson (1987), Henry Tresca (1878) observed hot lines in the form of a cross during hot forging of a platinum bar. Tresca pointed out that these were the lines of greatest sliding, and also therefore the zones of greatest development of heat. Subsequently, Massey (1921) reported the appearance of these hot lines during the hot forging of a metal at a relatively low temperature of 680°C. Massey noted that "when diagonal 'slipping' takes place there is great friction between particles and a considerable amount of heat is generated". The research activity in this area has increased significantly since the time Zener and Hollomon (1944) reported 32 μm wide shear bands during the punching of a hole in a steel plate and attributed this to the destabilizing effect of thermal softening in reducing the slope of the stress–strain curve in nearly adiabatic deformations. The hot lines of Tresca and Massey are now referred to as shear bands. Most of the analytical (Recht, 1964; Staker, 1981; Clifton, 1980; Molinari and Clifton, 1987; Burns, 1985; Wright, 1987; Anand *et al.*, 1987; Bai, 1981; Coleman and Hodgdon, 1985) and numerical (Clifton *et al.*, 1984; Merzer, 1982; Wu and Freund, 1984; Wright and Batra, 1985, 1987; Wright and Walter, 1987; Batra, 1987a, 1988) works aimed at understanding factors that enhance or inhibit the initiation and growth of shear bands have involved analyzing overall simple shearing deformations of a viscoplastic block. A material defect has been modeled by introducing (i) a temperature perturbation, (ii) a geometric defect such as a notch or a smooth variation in the thickness of the specimen, or (iii) assuming that the material at the site of the defect is weaker than the surrounding material. The experimental observations of Moss (1981), Costin *et al.* (1979), Hartley *et al.* (1987) and of Marchand and Duffy (1988) have contributed significantly to our understanding of the initiation and growth of shear bands in steels deformed at high strain rates.

Recently, LeMonds and Needleman (1986a,b), Needleman (1989), Batra and Liu (1989, 1990), Anand *et al.* (1988), Zhu and Batra (1990) and Batra and Zhang (1990) studied the phenomenon of shear banding in plane strain deformations of a viscoplastic solid. Whereas Needleman (1989) studied a purely mechanical problem, other works have treated a coupled thermomechanical problem. We note that LeMonds and Needleman and Anand *et al.* neglected the effect of inertia forces on the ensuing deformations of the body. In all of these works the entire body or the portion of the body whose deformations were analyzed had only one defect in it.

Here we study the plane strain thermomechanical deformations of a thermally softening viscoplastic solid containing an elliptical void and two thin layers placed symmetrically about the horizontal centroidal axis. These horizontal layers may be thought of as representing planes of chemical inhomogeneity. The voids can form during manufacturing. However, the symmetrical situation considered herein is to simplify the problem. The constitutive relations for the matrix material and the material of the thin layers are the same, except that the flow stress for the material of the thin layer in a quasistatic simple compression test equals either five times or one-fifth that of the matrix material. The points on the free edges where the thin layer and the matrix materials meet, as well as the void vertices on the major axes of the ellipsoid, act as nuclei for the initiation of shear bands. It thus becomes an interesting exercise to investigate where the shear bands initiate first and the interaction amongst them. We note that the problem formulation incorporates the effect of inertia forces, strain-rate sensitivity and heat conduction. However, the overall deformations of the body are assumed to be adiabatic. The nonlinear partial differential equations expressing the balance of mass, linear momentum and internal energy are solved numerically for a prescribed set of initial and boundary conditions.

2. FORMULATION OF THE PROBLEM

We use a fixed set of rectangular Cartesian coordinate axes to study the plane strain deformations of a thermally softening viscoplastic body being deformed in simple compression. The cross-section of the body, shown in Fig. 1, has an ellipsoidal void at the center and two thin layers of a different viscoplastic material placed symmetrically about the horizontal axis. The deformations of the body are assumed to be symmetrical about the two centroidal axes. Accordingly, only the deformations of the material in the first quadrant
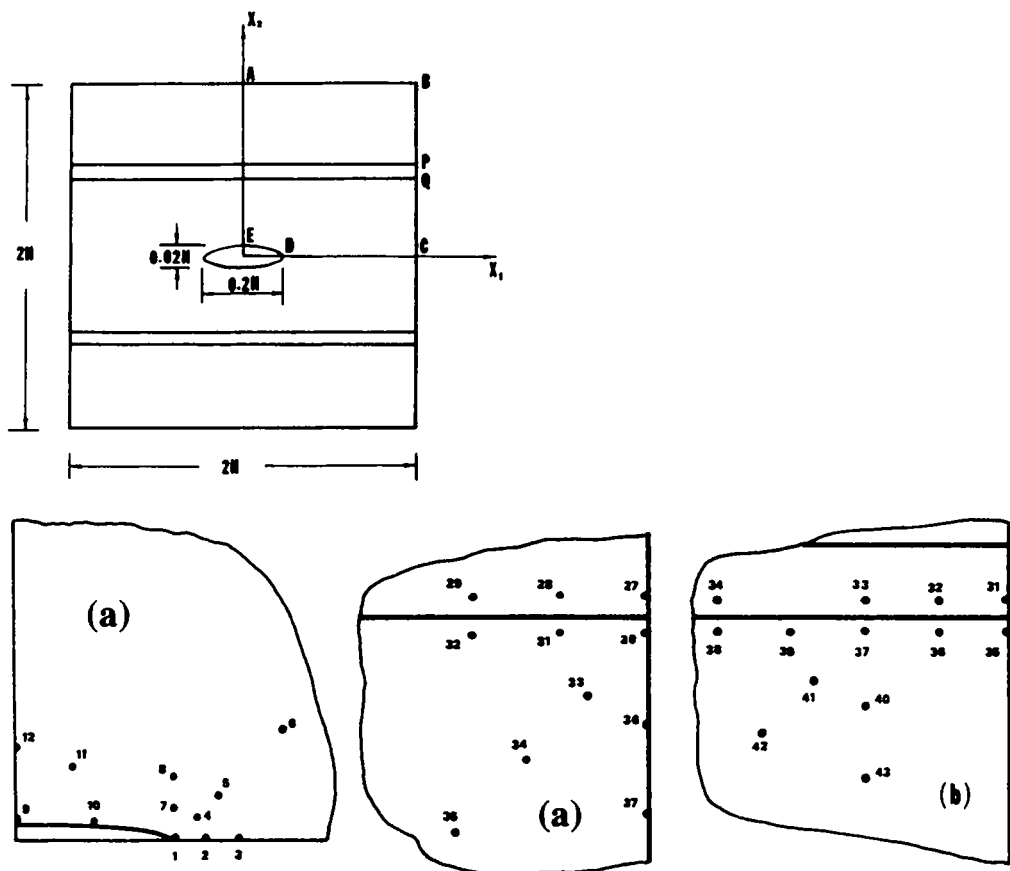

Fig. 1. The cross-section of the prismatic body studied. (a) Location of points for Figs 3 through 5. (b) Location of points for Fig. 8.

are analyzed. Equations governing these deformations are:

$$(\rho J)^{\cdot} = 0,\tag{1}$$

$$\rho_0 \dot{v}_i = T_{i\alpha,\alpha},\tag{2}$$

$$\rho_0\,\dot{e} = -Q_{\alpha,\alpha} + T_{i\alpha}v_{i,\alpha}.\tag{3}$$

Equations (1), (2) and (3) express, respectively, the balance of mass, linear momentum and internal energy. Here ρ is the present mass density of a material particle whose mass density in the reference configuration is ρ_0, J is the determinant of the deformation gradient $x_{i,\alpha}$, v_i the velocity of a material particle in the x_i-direction, x_i gives the position at time t of the material particle X_α, $T_{i\alpha}$ is the first Piola–Kirchoff stress tensor, e is the specific internal energy, Q_α is the heat flux measured per unit area in the reference configuration, and

$$D_{ij} = (v_{i,j} + v_{j,i})/2\tag{4}$$

is the strain-rate tensor. Furthermore, a superimposed dot indicates material time derivative, a comma followed by index $\alpha(j)$ implies partial differentiation with respect to X_α (x_j), and a repeated index implies summation over the range of the index.

The balance laws are supplemented by the following constitutive relations:

$$T_{i\alpha} = (\rho_0/\rho)\sigma_{ij}X_{\alpha,j}, \quad \sigma_{ij} = -B(\rho/\rho_0 - 1)\delta_{ij} + 2\mu D_{ij},\tag{5}$$

$$2\mu = [\sigma_0/\sqrt{3}I](1 + bI)^m(1 - \alpha\theta),\tag{6}$$

$$I^2 = (1/2)\bar{D}_{ij}\bar{D}_{ji},\tag{7}$$

$$\bar{D}_{ij} = D_{ij} - (1/3)D_{kk}\delta_{ij},\tag{8}$$

$$Q_\alpha = (\rho_0/\rho)q_iX_{\alpha,i}, \quad q_i = -k\theta_{,i},\tag{9}$$

$$\dot{e} = c\dot{\theta} + B(\rho/\rho_0 - 1)\dot{\rho}/\rho^2.\tag{10}$$

In these equations, the material parameter B may be regarded as the bulk modulus, σ_0 is the yield stress in a quasistatic simple compression test, parameters b and m describe the strain-rate hardening of the material, α is the thermal softening parameter, θ equals the temperature change of a material particle from that in the reference configuration, k is the thermal conductivity and c is the specific heat. Both k and c are taken to be constants and we have neglected stresses caused by the thermal expansion.

Equations (1) through (10) hold in the regions occupied by the matrix and the layer, the only difference being either

$$\sigma_0 \text{ layer} = 5\sigma_0 \text{ matrix}\tag{11a}$$

or

$$\sigma_0 \text{ layer} = (1/5)\sigma_0 \text{ matrix}.\tag{11b}$$

The values of other material parameters are the same for the matrix and the layer.

Define s by

$$\mathbf{s} = \boldsymbol{\sigma} + [B(\rho/\rho_0 - 1) - (2\mu/3) \text{ tr } \mathbf{D}]\mathbf{1},\tag{12a}$$

$$= 2\mu\bar{\mathbf{D}}.\tag{12b}$$

Equations (12), (5) and (6) give

$$(1/2 \text{ tr } \mathbf{s}^2)^{1/2} = (\sigma_0/\sqrt{3})(1 - \alpha\theta)(1 + bI)^m\tag{13}$$

which can be regarded as the equation of a generalized von Mises yield surface when the flow stress, given by the right-hand side of (13), at a material particle depends upon its strain rate and temperature. Alternatively, equation (5) can be interpreted as representing a non-Newtonian fluid whose viscosity depends upon the strain rate and temperature.

We introduce non-dimensional variables as follows:

$$\bar{\sigma} = \sigma/\sigma_0, \quad \bar{s} = s/\sigma_0, \quad \bar{B} = B/\sigma_0, \quad \bar{T} = T/\sigma_0,$$

$$\dot{\gamma}_0 = v_0/H, \quad \bar{t} = t\dot{\gamma}_0, \quad \bar{b} = b\dot{\gamma}_0,$$

$$\theta_0 = \sigma_0/(\rho_0 c), \quad \bar{\theta} = \theta/\theta_0, \quad \bar{\alpha} = \alpha\theta_0,$$

$$\bar{x} = x/H, \quad \bar{\rho} = \rho/\rho_0, \quad \beta = k/(\rho_0 c\dot{\gamma}_0 H^2). \tag{14}$$

Here $2H$ is the height of the block and v_0 is the velocity imposed on its top and bottom surfaces. Substituting for σ_{ij}, q_i and e from (5) through (10) into the balance laws (1) through (3), rewriting these in terms of non-dimensional variables, and dropping the superimposed bars, we arrive at the following set of nonlinear coupled field equations for ρ, v_i and θ:

$$(\rho J)^\cdot = 0, \tag{15}$$

$$\rho\nu\dot{v}_i = -B\rho_{,i} + [(1/\sqrt{3}I)(1+bI)^m(1-\alpha\theta)D_{ij}]_{,j}, \tag{16}$$

$$\rho\dot{\theta} = \beta\theta_{,ii} + (1/\sqrt{3}I)(1-\alpha\theta)(1+bI)^m \bar{D}_{ij}\bar{D}_{ij}, \tag{17}$$

where $\nu = \rho_0 v_0^2/\sigma_0$ is a non-dimensional number. The value of ν signifies the effect of inertia forces relative to the flow stress of the material. For the initial conditions we take

$$\rho(\mathbf{x}, 0) = 1, \quad \mathbf{v}(\mathbf{x}, 0) = \mathbf{0}, \quad \theta(\mathbf{x}, 0) = 0. \tag{18}$$

That is, the body is initially at rest at a uniform temperature and has constant mass density. The pertinent boundary conditions for the material analyzed in the first quadrant are

$$v_2 = -h(t), \quad T_{12} = 0 \quad \text{and} \quad Q_2 = 0, \quad \text{on the top surface AB}, \tag{19}$$

$$T_{11} = 0, \quad T_{21} = 0 \quad \text{and} \quad Q_1 = 0, \quad \text{on the right surface BC}, \tag{20}$$

$$v_2 = 0, \quad T_{12} = 0 \quad \text{and} \quad Q_2 = 0, \quad \text{on the bottom surface CD}, \tag{21}$$

$$T_{i\alpha}N_\alpha = 0 \quad \text{and} \quad Q_\alpha N_\alpha = 0, \quad \text{on the surface DE of the void}, \tag{22}$$

$$v_1 = 0, \quad T_{21} = 0 \quad \text{and} \quad Q_1 = 0, \quad \text{on the left surface EA}. \tag{23}$$

These boundary conditions simulate the situation when the top surface is moving downward with a speed $h(t)$, there is no friction between it and the loading device, the right surface is traction free, the void has not coalesced and the entire boundary is thermally insulated. The boundary conditions (21) and (23) are due to the presumed symmetry of the deformations about the x_1 and x_2 axes. When and where the void coalesces, boundary condition (22) is replaced by (21). For the loading function $h(t)$, we take

$$h(t) = t/0.005, \quad 0 \leqslant t \leqslant 0.005,$$

$$= 1, \quad t \geqslant 0.005. \tag{24}$$

At the common interface between the matrix and the reinforcing layer, the velocity field, surface tractions, the temperature and the normal component of the heat flux are assumed to be continuous.

3. COMPUTATION AND DISCUSSION OF RESULTS

3.1. Computational aspects

We use the updated Lagrangian method [e.g. see Bathe (1982)] to solve the problem. That is, in order to find the deformations of the body at time $t+\Delta t$, the configuration of the body at time t is taken as the reference configuration. The field equations (15) through (17) and the associated boundary conditions (19) through (23) are first reduced to a set of coupled nonlinear ordinary differential equations by using the Galerkin method and the lumped mass matrix [e.g. see Hughes (1987)]. For this purpose, the spatial discretization of the domain consisting of four-noded isoparametric quadrilateral elements is employed. Figure 2 depicts the mesh used in the reference configuration. The number of ordinary
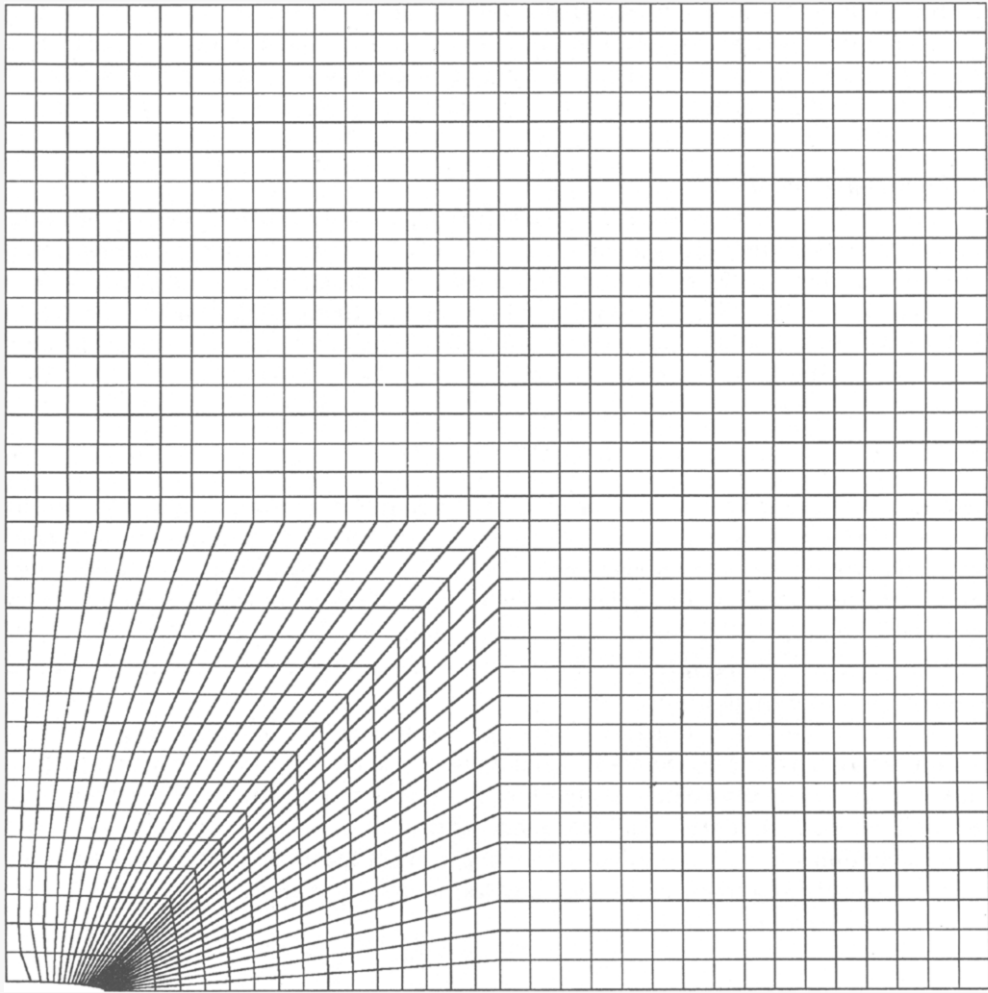
Fig. 2. The finite element discretization of the domain analyzed.

differential equations equals four times the number of nodes because at each node, the mass density, the two components of the velocity and the temperature are unknown. The initial conditions (18) imply that the initial mass density at each node point equals one, and the initial values of the two velocity components and the temperature equal zero at all nodes.

These ordinary differential equations are integrated by using the IMSL subroutine LSODE. In the subroutine, the option to integrate a stiff set of equations is employed. The subroutine adjusts the time step adaptively until a solution of the coupled nonlinear differential equations has been computed to the desired accuracy.

The finite element code developed earlier by Batra and Liu (1989) has been modified to study the present problem. After each time increment, the new surface of the void is computed and examined to see if any node on the void surface has either reached or crossed the horizontal axis of symmetry. If a node on the void surface has crossed the horizontal axis, computations are repeated from the previously computed solution but with a smaller value of the time step. As soon as a node on the void surface reaches the horizontal axis, the boundary conditions on the node are changed to those given by (21).

In the results presented below, we have used the following values of various material and geometric parameters:

$$b = 10,000\,\text{s}, \quad \sigma_0 = 333\,\text{MPa}, \quad k = 49.22\,\text{W}\,\text{m}^{-1}\,{}^\circ\text{C}^{-1}, \quad m = 0.025,$$

$$c = 473\,\text{J}\,\text{kg}^{-1}\,{}^\circ\text{C}^{-1}, \quad \rho_0 = 7860\,\text{kg}\,\text{m}^{-3}, \quad B = 128\,\text{GPa},$$

$$H = 5\,\text{mm}, \quad v_0 = 25\,\text{m}\,\text{s}^{-1}, \quad \alpha = 0.0025\,{}^\circ\text{C}^{-1}. \tag{25}$$

Thus the average applied strain rate equals $5000 \, s^{-1}$, $\theta_0 = 89.6^\circ C$ and $v = 0.015$. We note that in the simple shearing problem, Batra (1988) observed that the inertia forces play a noticeable role when $v = 0.004$. Hence, the inertia forces will very likely play a significant role in the present problem.

3.2. Discussion of results

3.2.1. *Layer material stronger than the matrix material.* In order to understand which points in the body are deforming severely, we have plotted the development of the maximum principal logarithmic strain ε, the temperature rise θ and the effective stress s_e, equal to the right-hand side of eqn. (13), at several material points near the major and minor axes of the ellipsoidal void and at points where the "reinforcing layer" and the matrix material meet. The logarithmic strain ε is defined as

$$\varepsilon = \ln \lambda_1 \simeq -\ln \lambda_2 \tag{26}$$

where λ_1^2 and λ_2^2 are the eigenvalues of the right Cauchy–Green tensor $C_{\alpha\beta} = x_{i,\alpha} x_{i,\beta}$ or the left Cauchy–Green tensor $B_{ij} = x_{i,\alpha} x_{j,\alpha}$. The equality in the second relation in (26) holds because the deformations are nearly isochoric, i.e. $\lambda_1 \lambda_2 = 1$. Figures 3a, 3b and 3c depict, respectively, the evolution of ε, θ and s_e at eight material points near the major axis of the ellipsoidal void and also at a material point far removed from it. The coordinates, in the stress free reference configuration, of these points are given in the figure captions and their approximate locations are shown in Fig. 1a. The material points 1, 2 and 3 are a little bit off of the horizontal axis, points 1, 4, 5 and 6 lie on a straight line making an angle of nearly 45° with the horizontal axis, points 1, 7 and 8 are on an almost vertical line, and point 13 is near the horizontal centroidal axis but far removed from the void tip. The temperature rise θ and the maximum principal logarithmic strain ε at point 13 increase very slowly as the block continues to be compressed. The temperature at the other eight points considered rises rapidly in the beginning and then increases slowly. The values of ε at points 1 and 2
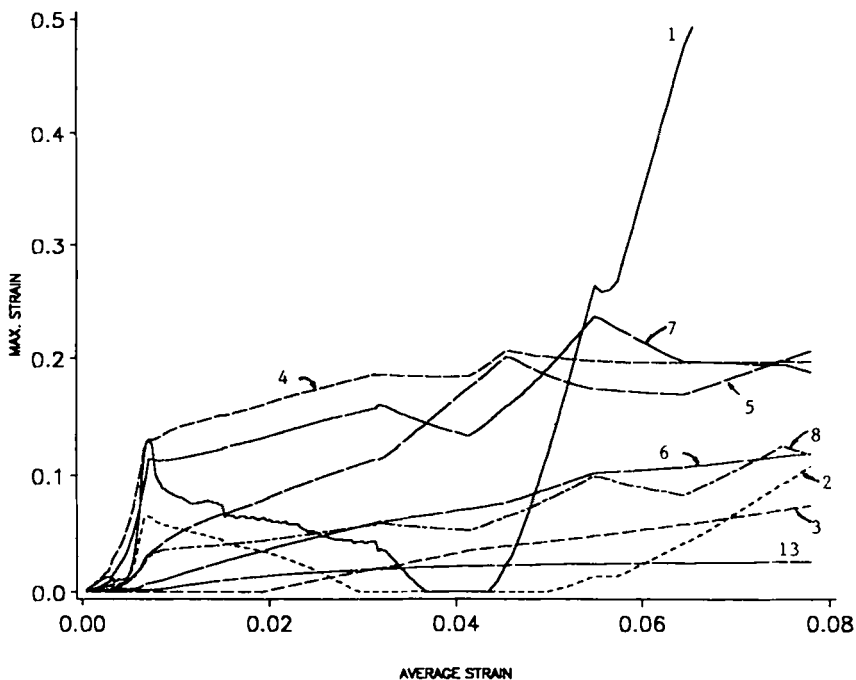

Fig. 3a. The maximum principal logarithmic strain versus the average strain at points 1, 2, 3, 4, 5, 6, 7, 8 and 13. Coordinates, in the stress free reference configuration, of these points are: 1(0.1001, 0.0001), 2(0.1200, 0.0001), 3(0.1400, 0.0001), 4(0.1141, 0.0141), 5(0.1283, 0.0283), 6(0.1707, 0.0707), 7(0.1001, 0.0200), 8(0.1001, 0.0400), 13(0.8001, 0.0001).
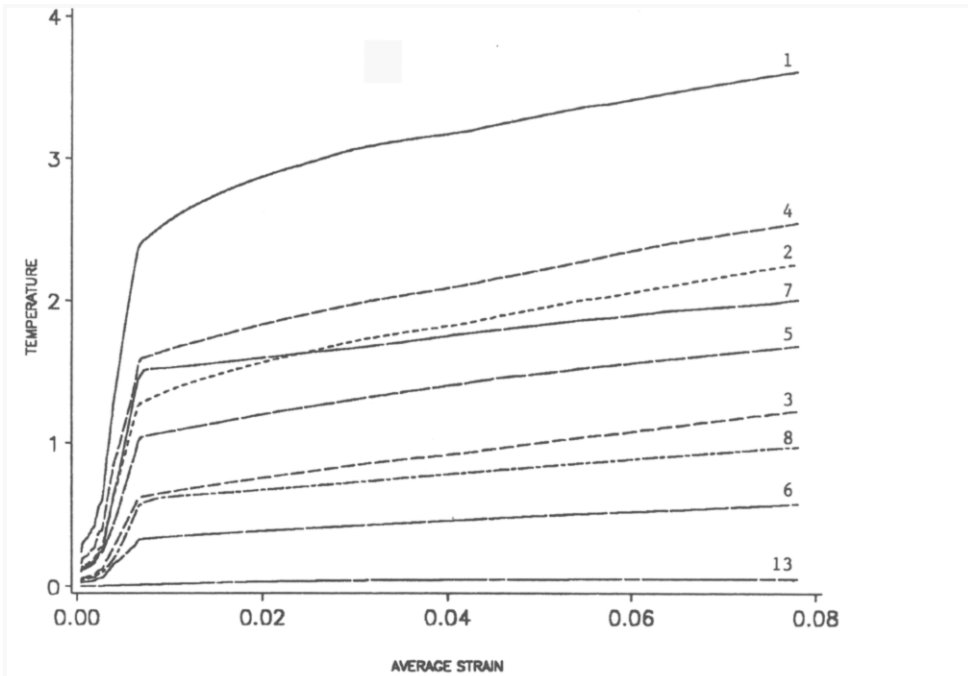
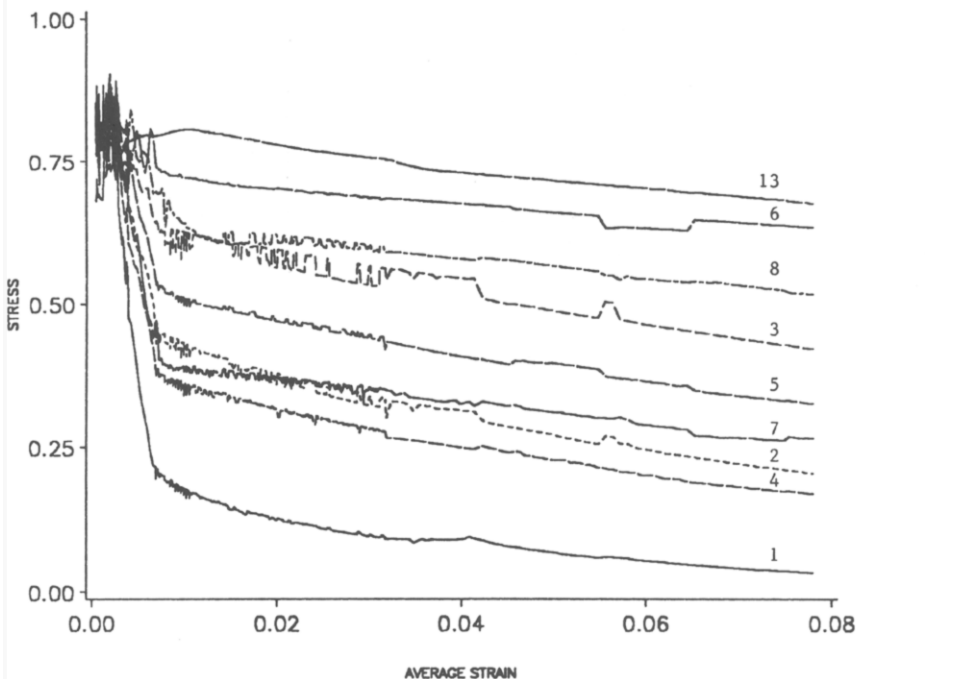Fig. 3b. The temperature rise versus the average strain at points 1 through 8, and 13.

Fig. 3c. The effective stress versus the average strain at points 1 through 8, and 13.

near the void tip increase at first and the consequent temperature rise makes the material surrounding these points softer. The severe deformations of this material make the void coalesce. This is indicated by the drop in the value of ε at point 1. The coalescence of the void results in a redistribution of deformations in the material surrounding point 1. The rapid growth of ε at the void tip (point 1) when the average strain equals 0.044 is indicative of the eventual development of the shear band there. The plot of the effective stress in Fig.

3c indicates that the effective stress at a material point is lower if its temperature is higher, in conformity with the constitutive relation employed. Even when the strain at material point 1 rises rapidly, the low value of the effective stress there gives rise to moderate values of the plastic working and the temperature rise does not increase significantly.

In Fig. 4, we have plotted the evolution of ε and θ at points 9, 10, 11, 12 and 13. The first four points are near the vicinity of the point where the void surface intersects the vertical axis. Both the temperature rise and the value of the maximum principal logarithmic

Fig. 4a. The maximum principal logarithmic strain versus the average strain at points 9 through 13. Coordinates, in the stress free reference configuration of these points are: 9(0.0001, 0.0101), 10(0.0500, 0.0101), 11(0.0354, 0.0454), 12(0.0001, 0.0601), 13(0.8001, 0.0001).
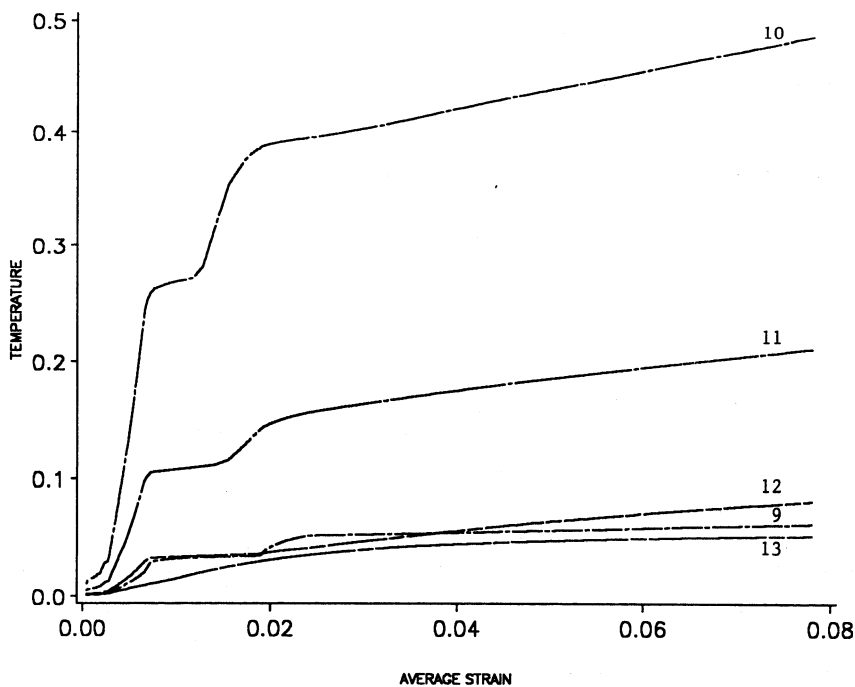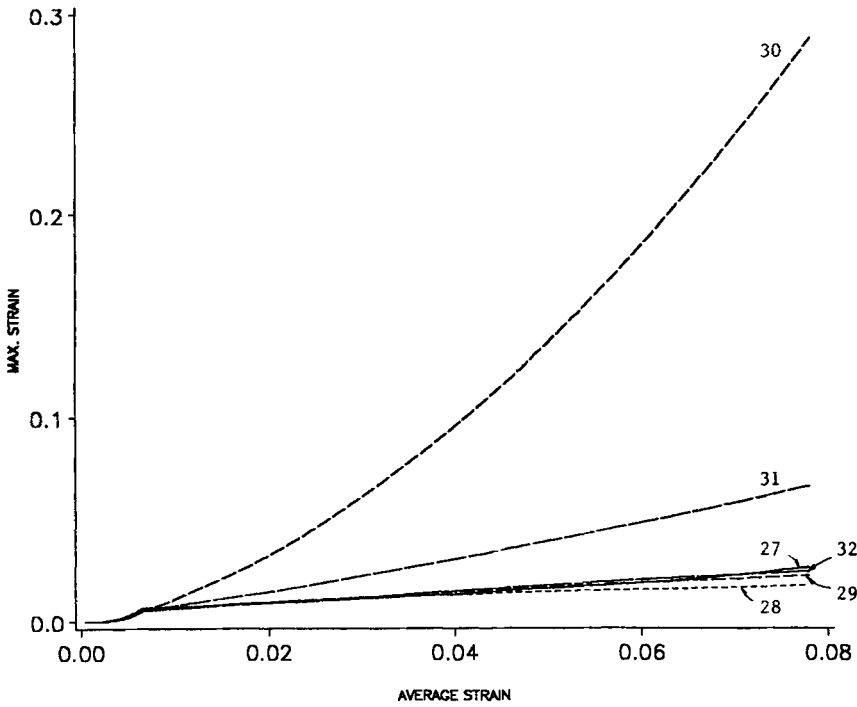

Fig. 4b. The temperature rise versus the average strain at points 9 through 13.

strain at these points are approximately an order of magnitude lower than those at point 1 near the void tip.

In order to delineate the difference between the deformations of the matrix material and the material of the hard layer, we show in Fig. 5a the evolution of ε at six points

Fig. 5a. The maximum principal logarithmic strain versus the average strain at points 27 through 32. Coordinates, in the stress free reference configuration, of these points are: 27(0.9999, 0.4850), 28(0.9500, 0.4850), 29(0.9000, 0.4850), 30(0.9999, 0.4650), 31 (0.9500, 0.4650), 32(0.9000, 0.4650).
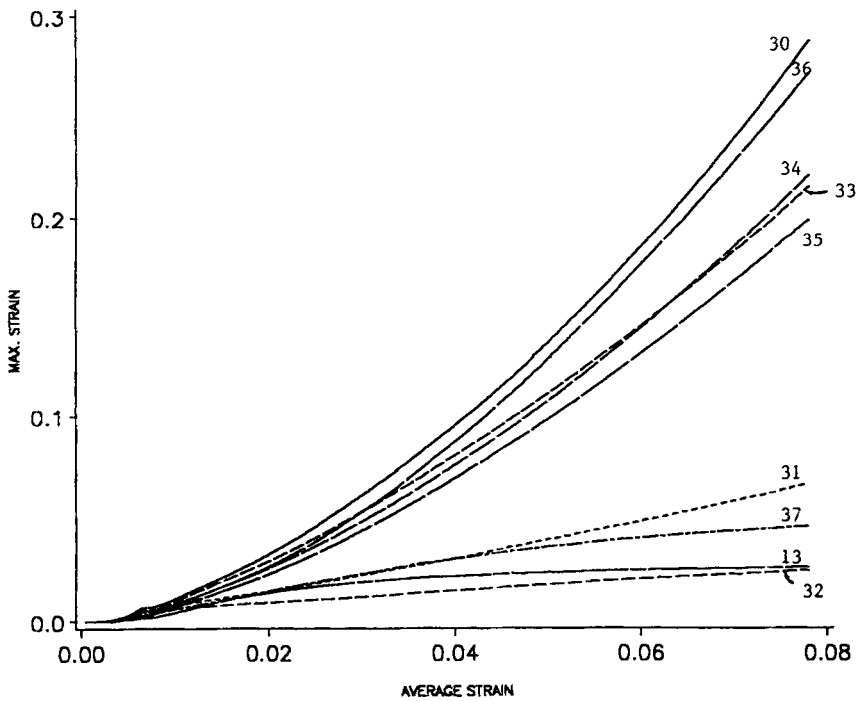

Fig. 5b. The maximum principal logarithmic strain versus the average strain at points 30 through 37, and point 13. Coordinates of points in the stress free reference configuration not given in previous figures are: 33(0.9645, 0.4296), 34(0.9293, 0.3943), 35(0.8939, 0.3589), 36(0.9999, 0.4150), 37(0.9999, 0.3650).

near the common interface between the matrix and the reinforcing layer. Points 27, 28 and 29 are in the layer and points 30, 31 and 32 are in the matrix. The deformation of points 27, 28, 29, 31 and 32 is miniscule as compared to that of point 30, whose deformation is comparable to that of the point near the void tip. Also the maximum principal logarithmic strain ε rises monotonically at point 30. Because of the very large values of the effective stress in the hard layer, the plastic working and the resulting temperature rise in it are more than that at adjoining points in the matrix material. Because of the larger deformations of the matrix material near point 30, eventually the temperature rise at point 30 exceeds that at point 27 in the hard layer. To explore the direction of propagation of the deformation from point 30, we have plotted in Fig. 5b the maximum principal logarithmic strain versus the average strain at points 30 through 37 and point 13. Points 30, 36 and 37 are on a vertical line near the right traction free surface, and points 30, 33, 34 and 35 are on a line that makes an angle of 45° with the vertical. The values of ε at points 31, 32 and 37 are comparable to that at point 13 in the matrix material. Recall that point 13 is near the horizontal centroidal axis and far removed from the void tip. The values of ε at points 31, 32 and 37 are considerably smaller than that at point 30, indicating thereby that the deformation ensuing at point 30 neither propagates horizontally nor vertically. The large values of ε at point 36 are indicative of the fact that a small material region surrounding point 30 is deforming severely. Since the values of ε at points 33, 34 and 35 are comparable to that at point 30 and generally decrease as we move away from point 30, we may conclude that the deformation propagates along the line joining these points, i.e. along the line making an angle of 45° with the vertical. The plots of ε at points situated near the upper interface between the reinforcing layer and the matrix material are similar to those at points 27 through 35 and are not included herein.
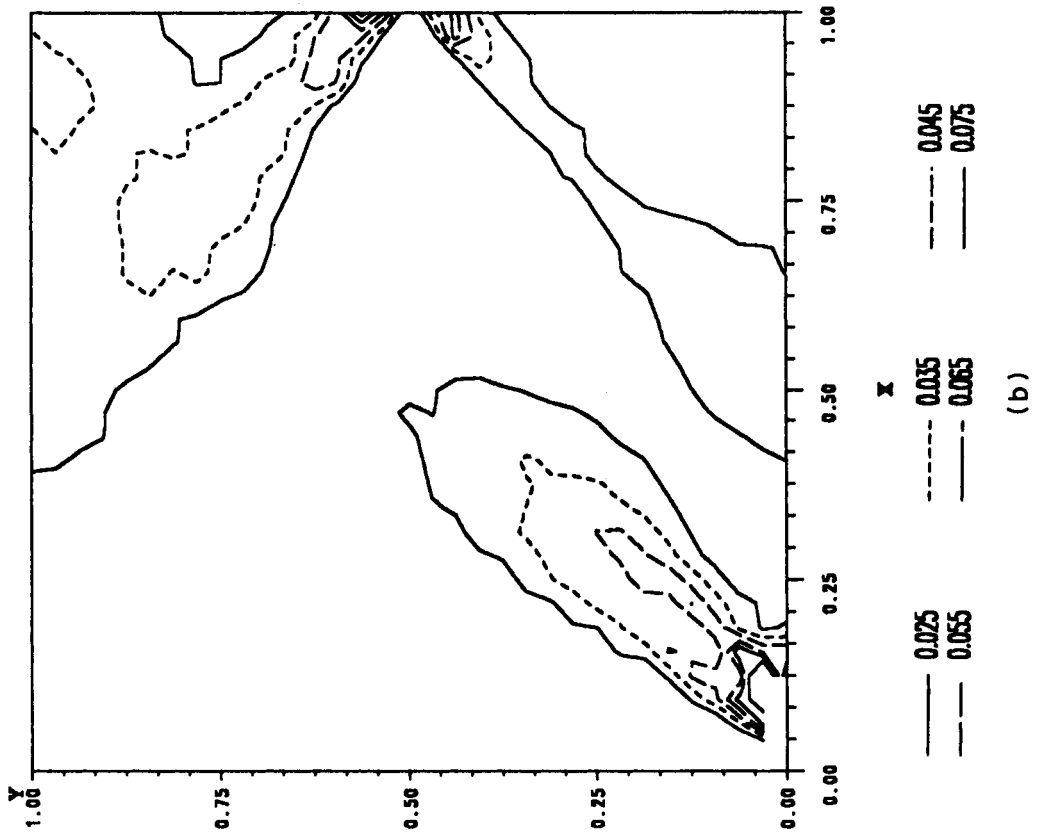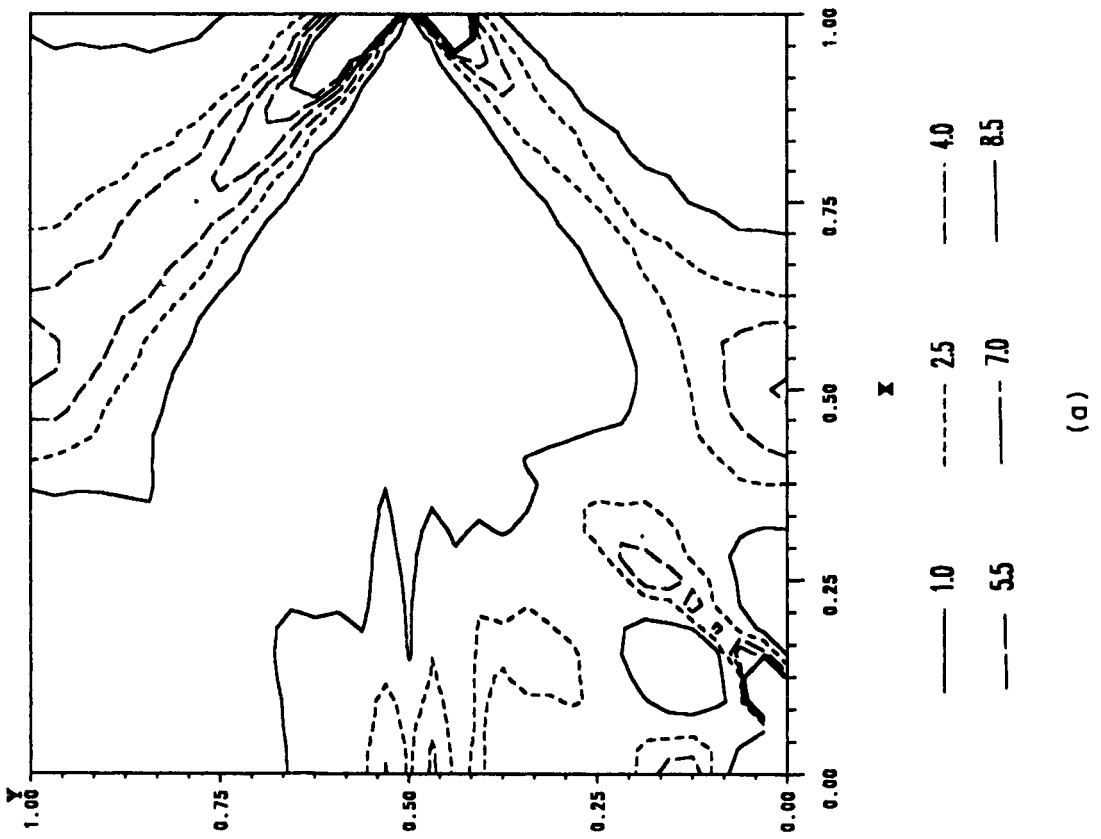
In order to elucidate the evolution of a shear band, we have plotted in Figs 6 and 7 contours of the second invariant I of the deviatoric strain-rate tensor $\tilde{D}$, the maximum principal logarithmic strain ε, and the temperature rise θ at two different values of the average strain. The contours of I describe how a material particle is deforming at a given instant, contours of ε give the accumulated deformation until that time, and contours of θ describe the total energy dissipated into heat till that time and the resulting temperature rise. We note that the contour plot routine interpolates the data at numerous points in the domain from that supplied at discrete points. Figure 6 shows the contours of I, ε and θ when $\gamma_{avg} = 0.0248$. It follows from the contours of I that the material near the void tip and points P and Q on the traction free right edge where the reinforcing layer meets it is deforming severely. As described earlier, these intense deformations propagate along lines inclined at $\pm 45°$ to the horizontal. The contours of ε and θ reveal that the material surrounding the aforestated lines has undergone severe deformations. Even though the strain rate and the strain in the layer are negligible as compared to their maximum values in the matrix material, the stress in the layer is high. Consequently, the plastic work done and the resulting temperature rise in the layer are not that small. The contours of I, ε and θ at an average strain of 0.0308 plotted in Fig. 7 are evidence of the narrowing down of the rapidly deforming region. Three bands, two initiating from points P and Q, and the third from the void tip, have formed. The maximum values of ε and θ equal 0.134 and 133°C, respectively. We note that if a block of rigid/perfectly plastic material with flow stress equal to 333 MPa were deformed homogeneously in simple compression to an average strain of 0.0308, the temperature rise would equal 2.6°C assuming that all of the plastic work done has been converted into heat. Thus, the significant temperature increase within the band signifies the intense deformation therein.

3.2.2. Layer material weaker than the matrix material.
We first investigate the development of shear bands initiating from points P and Q that are on the right traction free surface and the common interfaces between the layer and the matrix material. For this purpose, we have plotted in Fig. 8a the growth of the maximum principal logarithmic strain ε at points 31 through 38. Points 31, 32, 33 and 34 are on the layer side and points 35, 36, 37 and 38 are on the matrix side of the common interface between the layer and the matrix.

The first four points lie on a horizontal line in the layer, and the last four points lie on a different horizontal line in the matrix. Amongst these eight points, the growth of ε at point 31 is the maximum. The relative magnitude of ε at these points indicates that the severe deformation initiating from point 31 propagates horizontally to point 32 within the softer layer. Similarly, the severe deformation initiating from point Q propagates horizontally within the soft layer. Recall that in the previous case, the severe deformations occurred at the matrix particles on the common interface and propagated into the softer matrix material. Since the values of ε at point 34 are quite small as compared to that at points 31 and 32, the severe deformation either did not propagate horizontally from point 32 to point 34, or there was not enough time for it to arrive at point 34. Which one of these two alternatives is valid can be derived from the plots of ε at points 37 through 43. All of these points are in the matrix. Because the flow stress in a quasistatic simple compression test for the matrix material is five times that for the material of the layer, the strain rates and hence the strains in the matrix material are small relative to those in the layer. We note that points 37, 38 and 39 are on a horizontal line, 37, 40 and 43 are on a vertical line and 37, 41 and 42 are on a line that makes an angle of 45° with the vertical. For comparison purposes, the values of ε at point 13 which is near the horizontal centroidal axis and far removed from the ellipsoidal void are also plotted. The values of ε at these points indicate that the likely direction of propagation of the shear band from point 37 is along the line joining it to points 41 and 42. Similarly, the severe deformations initiating from point Q on the upper interface between the layer and the matrix material will propagate horizontally first into the soft layer and then into the matrix material along a line that makes an angle of 45° with the vertical line. In order to see whether these two bands propagate independently of each other or not, we have plotted in Fig. 9 the contours of the maximum principal logarithmic strain at successively increasing values of γ_{avg}. At $\gamma_{avg} = 0.013$, shear bands have initiated from the void tips on the major axis of the elliptical void as well as points on the free edge where the layer meets the matrix material. Whereas the band originating from points on the free edge propagates into the softer layer material, those initiating from the void tips propagate into the matrix. The two bands initiating from points P and Q essentially coalesce immediately into one because of the small thickness of the layer. Also due to the competing effect of the maximum shear stress in the $\pm 45°$ directions and the relatively negligible thickness of the layer, the band propagates horizontally into the layer.

When the body has been deformed to an average strain of 0.0177, the matrix material has softened somewhat because of its being heated up. The shear band originating from the void tip has propagated more into the matrix material. The two bands that had coalesced into one and were propagating horizontally into the layer now start to bifurcate and propagate into the matrix material in the directions of the maximum shear stress. This bifurcation of the shear band into two bands becomes clearer in Fig. 9c. At $\gamma_{avg} = 0.02053$, the shear band that initiated from the void tip has merged with the one that bifurcated from the band in the layer. The other band bifurcating from the one in the layer continues to travel in the $-45°$ direction into the matrix material. During subsequent deformations of the body, all bands propagate more into the matrix material. When $\gamma_{avg} = 0.0273$, the bands originating from the void tip and the one diverted out of the layer material have merged and propagated to the top right corner of the block. During the ensuing deformations, these bands do not quite narrow down into thin bands. Rather, the interaction among various bands broadens the region that has deformed severely. Figure 9g shows contours of the maximum principal logarithmic strain at $\gamma_{avg} = 0.0333$. The contour of $\varepsilon = 0.075$ has propagated significantly into the matrix material from the void tip and also into the softer layer and the surrounding matrix material near the points where the layer meets the traction free edge of the matrix. Note that the maximum value 0.40 of ε equals 12 times the average strain of 0.0333.

Figure 10 depicts the contours of the temperature at various values of γ_{avg}. We recall that the temperature rise at a point depends upon the total energy dissipated. At $\gamma_{avg} = 0.013$, even though the layer material near the free edge has deformed severely, it has not been heated up much because of the rather low value of stresses in it. The contours of temperature reinforce the picture given above of the growth of and the interaction among various bands.
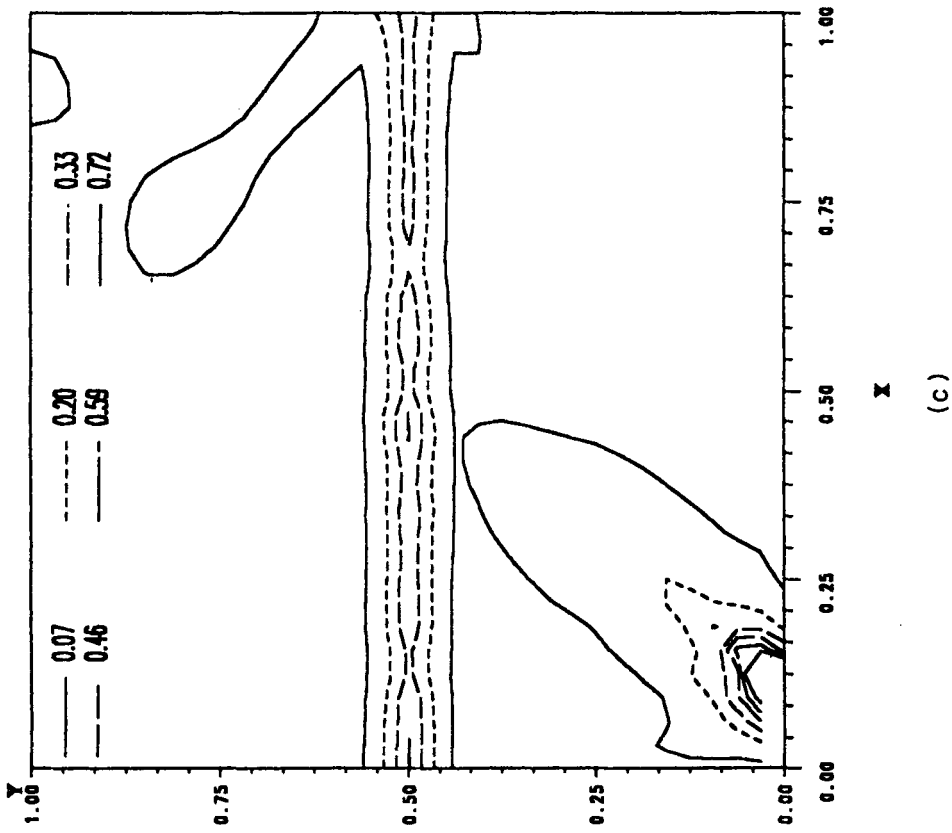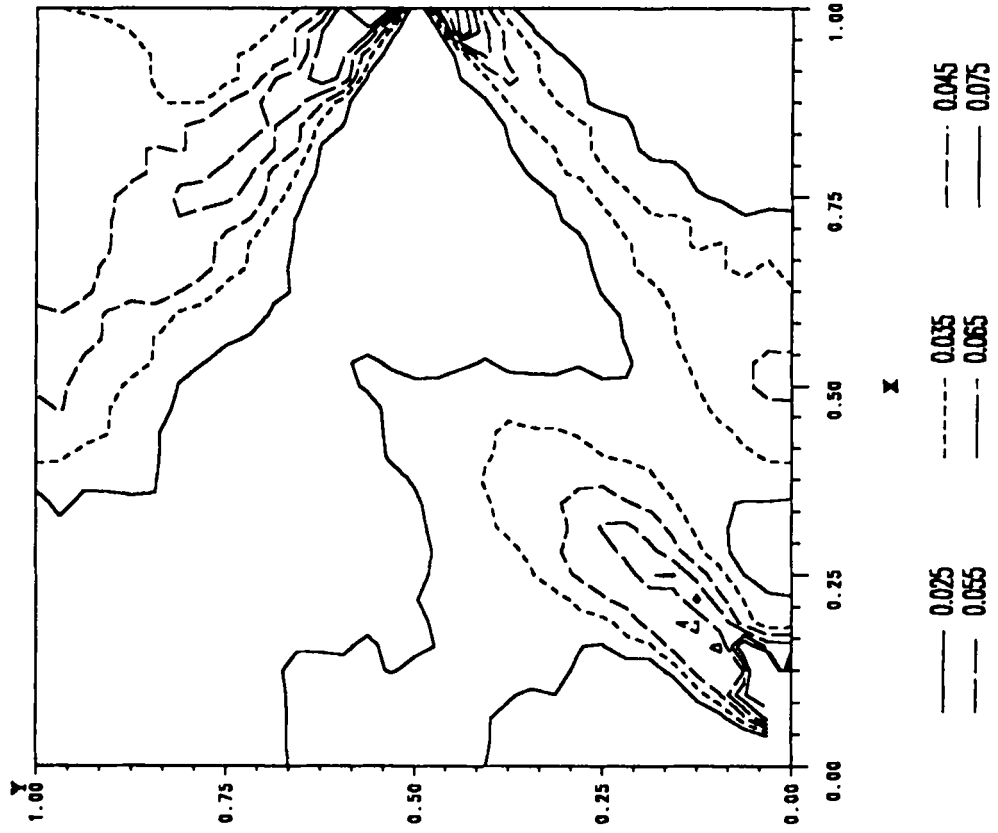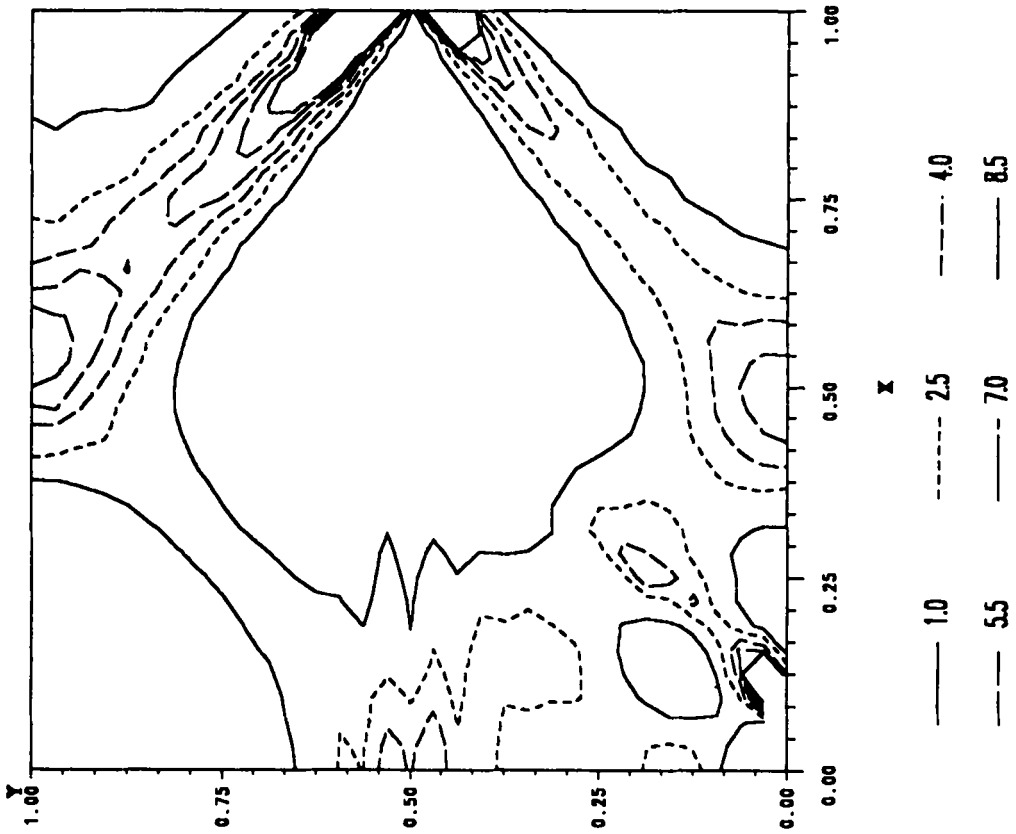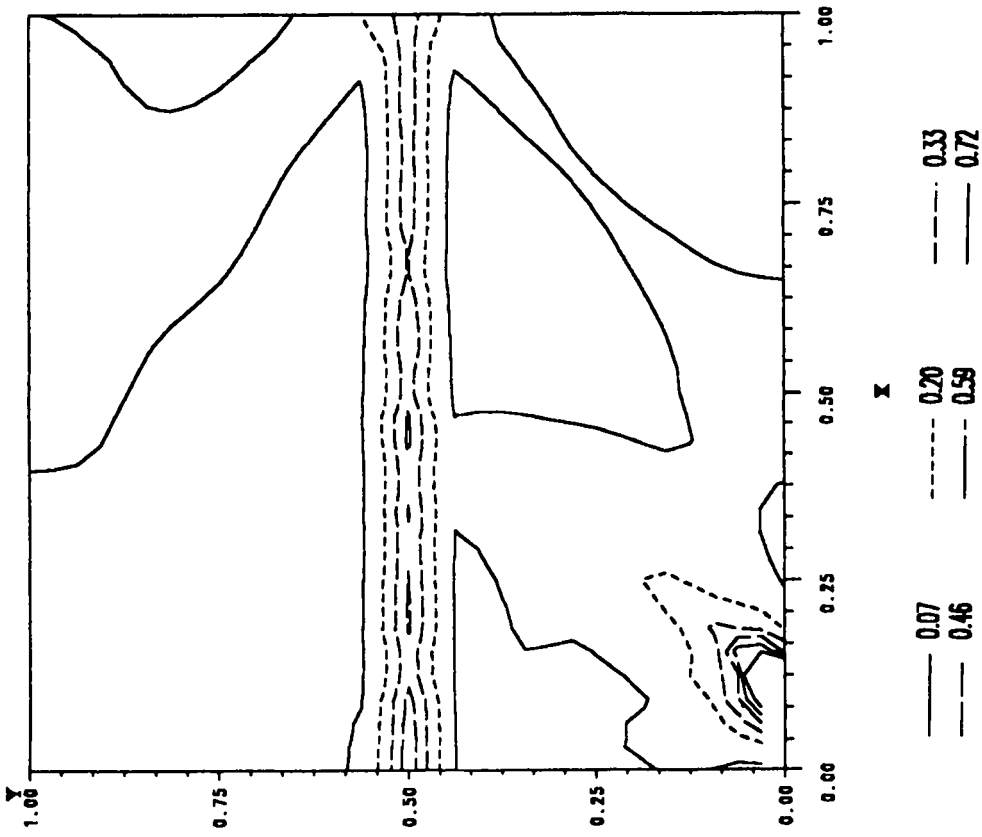
(a)

1.0 ——————   2.5 ------   4.0 — — —
5.5 — — —   7.0 — —   8.5 ——————

(b)

0.025 ——————   0.035 ------   0.045 — — —
0.055 — — —   0.065 — —   0.075 ——————

Fig. 6. Contours of (a) the second invariant I of the deviatoric strain-rate tensor, (b) the maximum principal logarithmic strain, and (c) the temperature rise at $\gamma_{avg} = 0.0248$ (σ_0 layer = $5\sigma_0$ matrix).
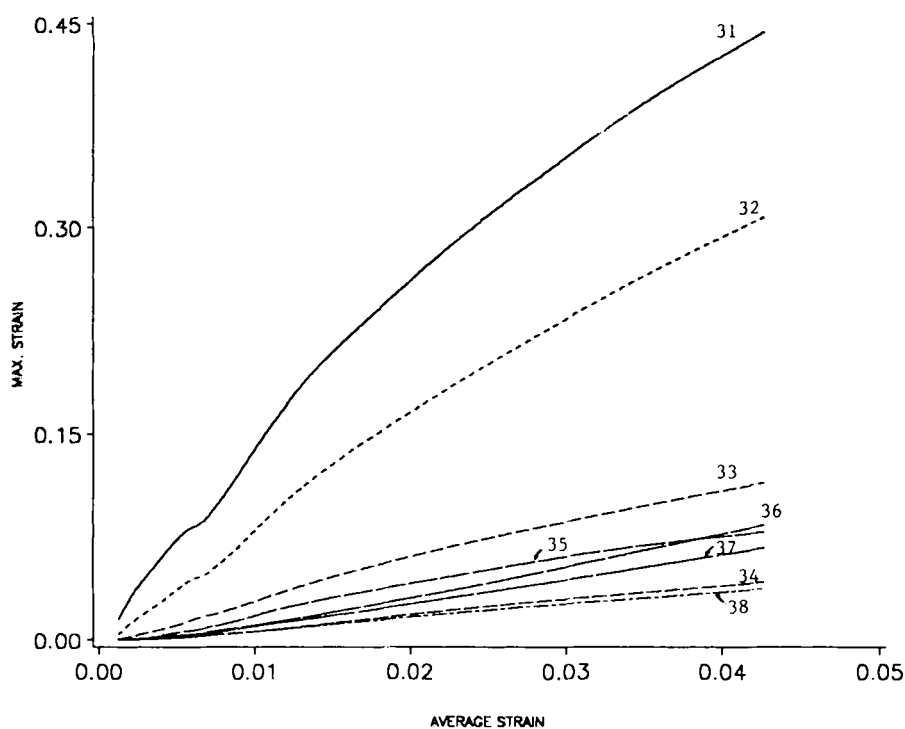
0.025   0.035   0.045
0.055   0.065   0.075

(b)

1.0   2.5   4.0
5.5   7.0   8.5

(a)

Fig. 7. Contours of (a) the second invariant I of the deviatoric strain-rate tensor, (b) the maximum principal logarithmic strain, and (c) the temperature rise at $\gamma_{avg} = 0.0308$ (σ_0 layer $= 5\sigma_0$ matrix).

Fig. 8a. The maximum principal logarithmic strain versus the average strain at points 31 through 38. Coordinates of these points in the stress free reference configuration are: 31(0.9999, 0.4850), 32(0.9450, 0.4850), 33(0.8900, 0.4850), 34(0.7800, 0.4850), 35(0.9999, 0.4650), 36(0.9450, 0.4650), 37(0.8900, 0.4650), 38(0.7800, 0.4650).

Fig. 8b. The maximum principal logarithmic strain versus the average strain at points 37 through 43. Coordinates of these points in the stress free reference configuration are: 39(0.8350, 0.4650), 40(0.8900, 0.4100), 41(0.8511, 0.4261), 42(0.8122, 0.3872), 43(0.8900, 0.3550).

Fig. 9. Contours of the maximum principal logarithmic strain at different values of γ_{avg} for the case when σ_0 layer $= (1/5)\sigma_0$ matrix. (a) $\gamma_{avg} = 0.013$, (b) $\gamma_{avg} = 0.0177$, (c) $\gamma_{avg} = 0.0205$, (d) $\gamma_{avg} = 0.0243$, (e) $\gamma_{avg} = 0.0273$, (f) $\gamma_{avg} = 0.0303$, (g) $\gamma_{avg} = 0.0333$.
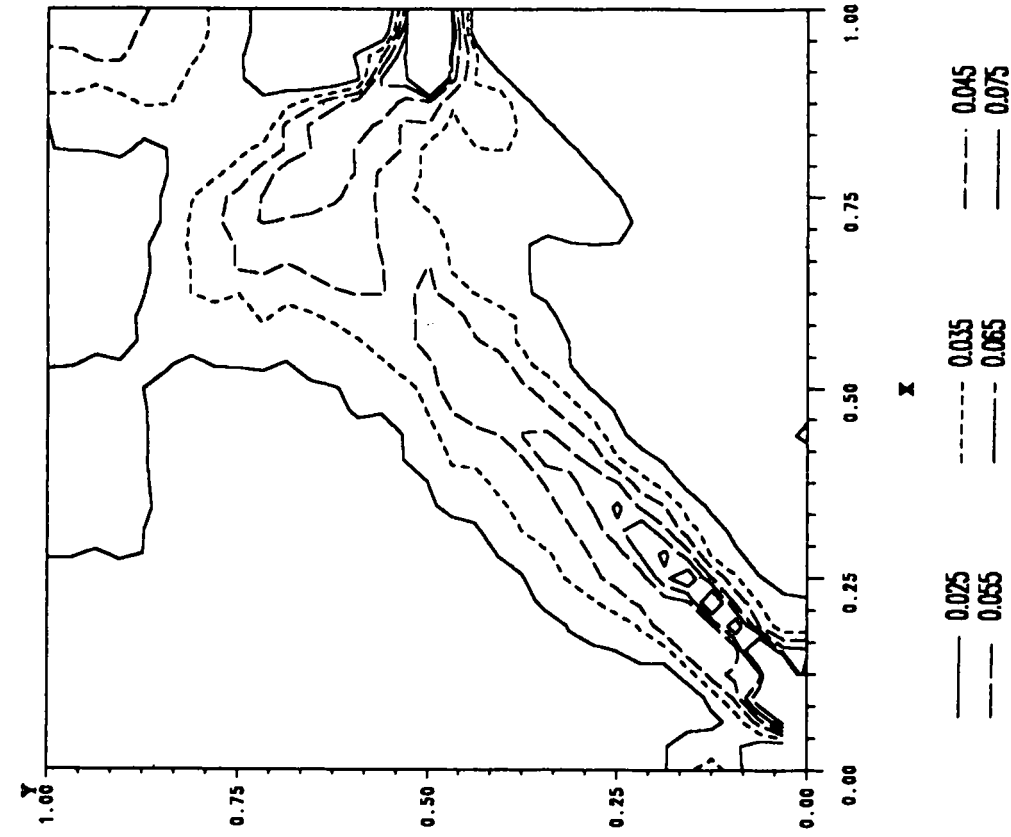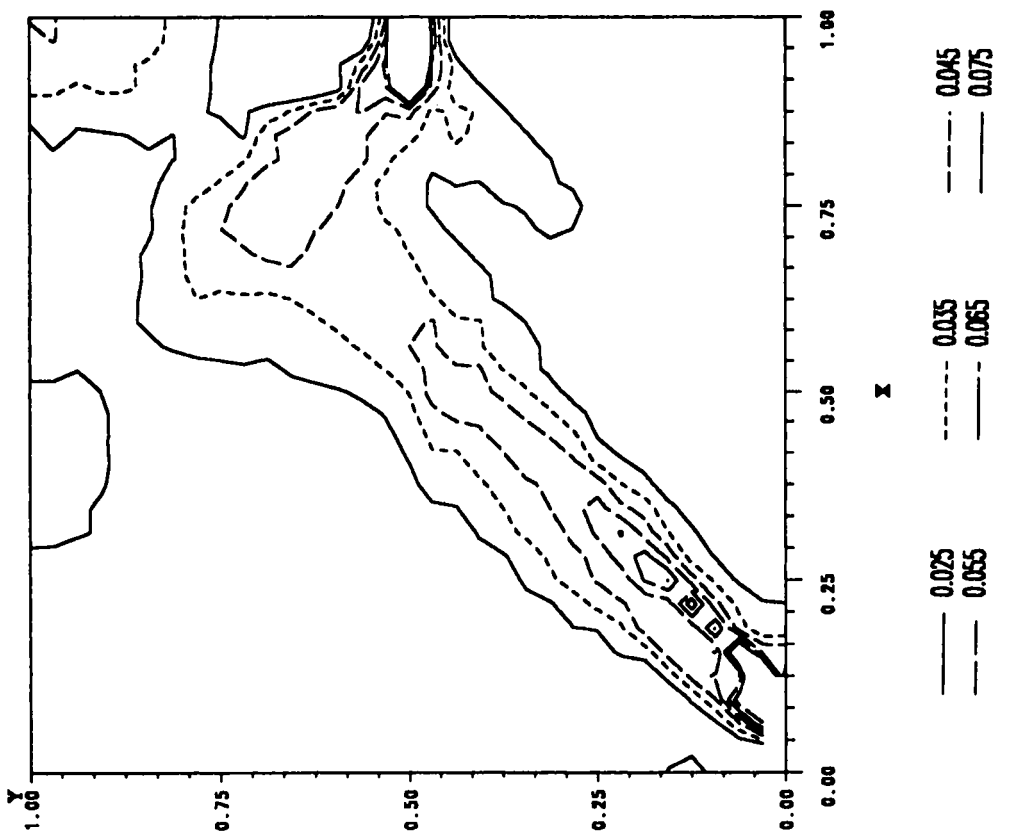
(Continued overleaf)

Fig. 9—continued.

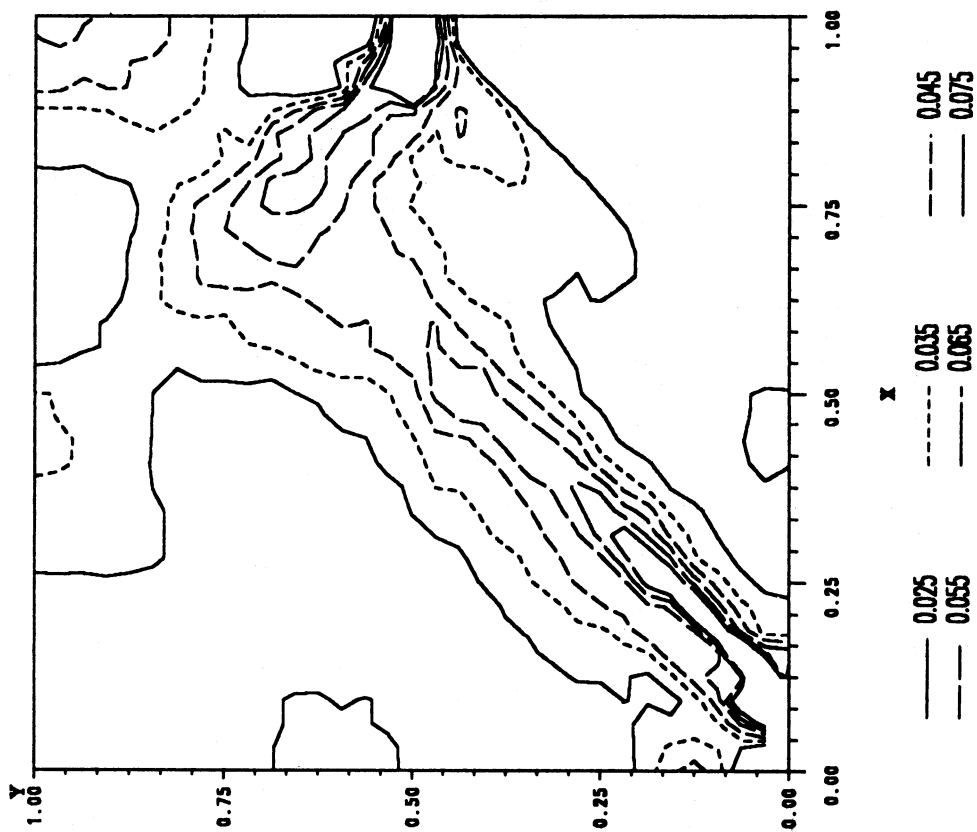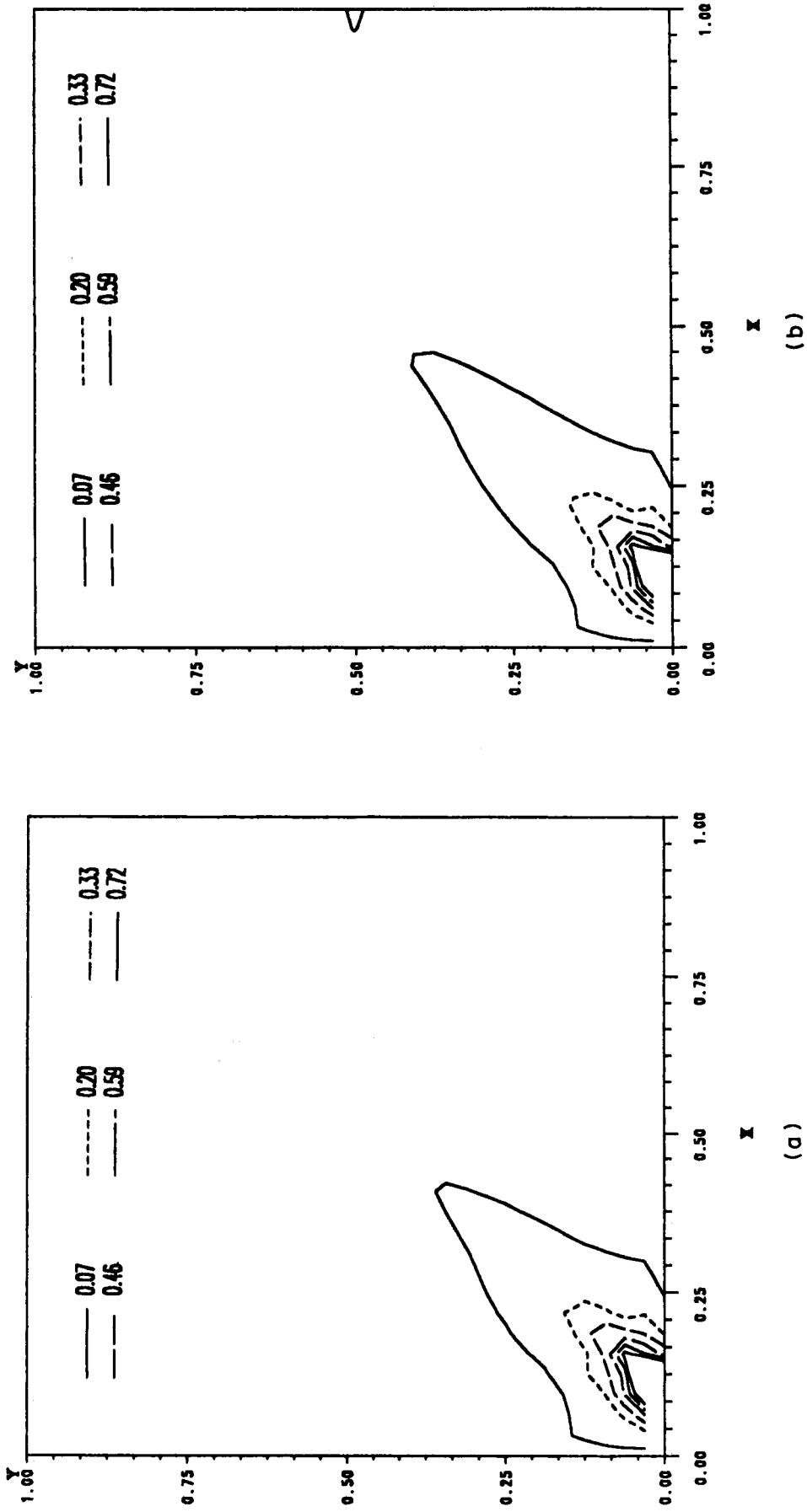Fig. 9—continued.

Fig. 9—continued.

Fig. 10. Contours of the temperature rise at different values of γ_{avg} for the case when σ_0 layer $= (1/5)\sigma_0$ matrix. See Fig. 9 for values of γ_{avg}.
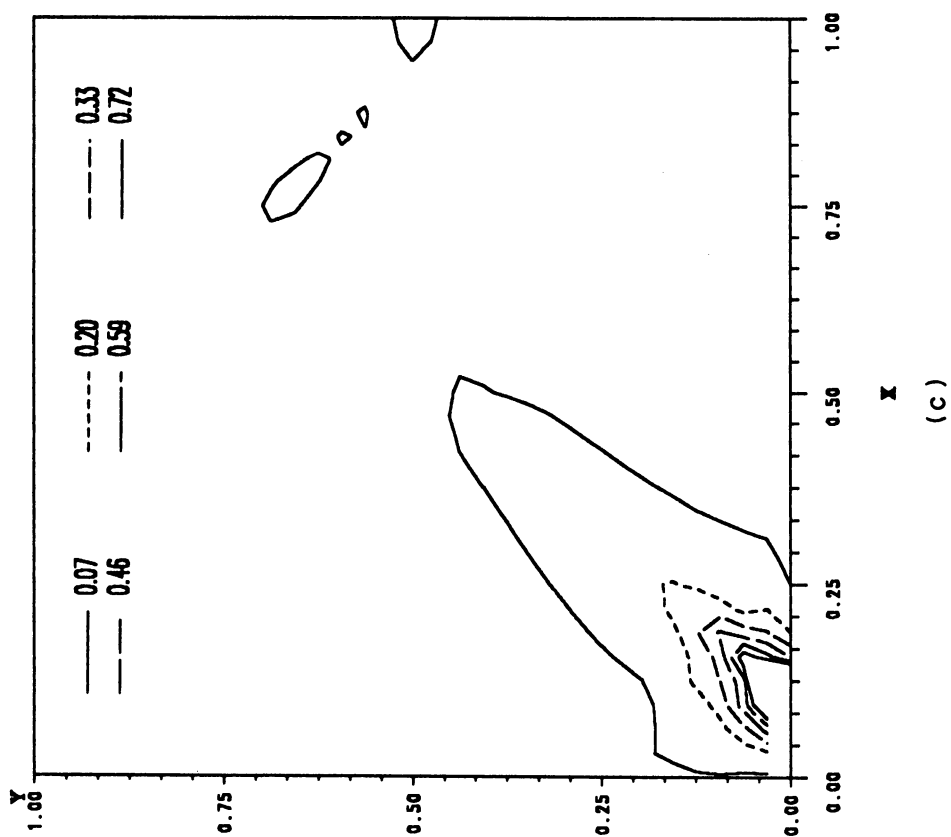
(Continued overleaf)
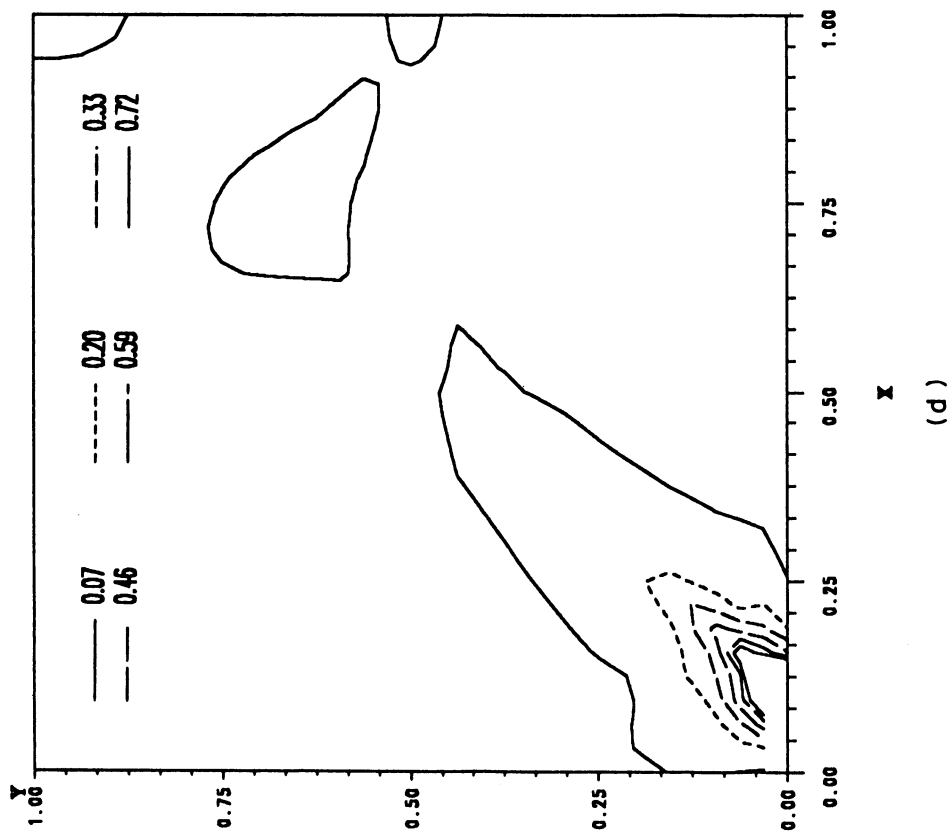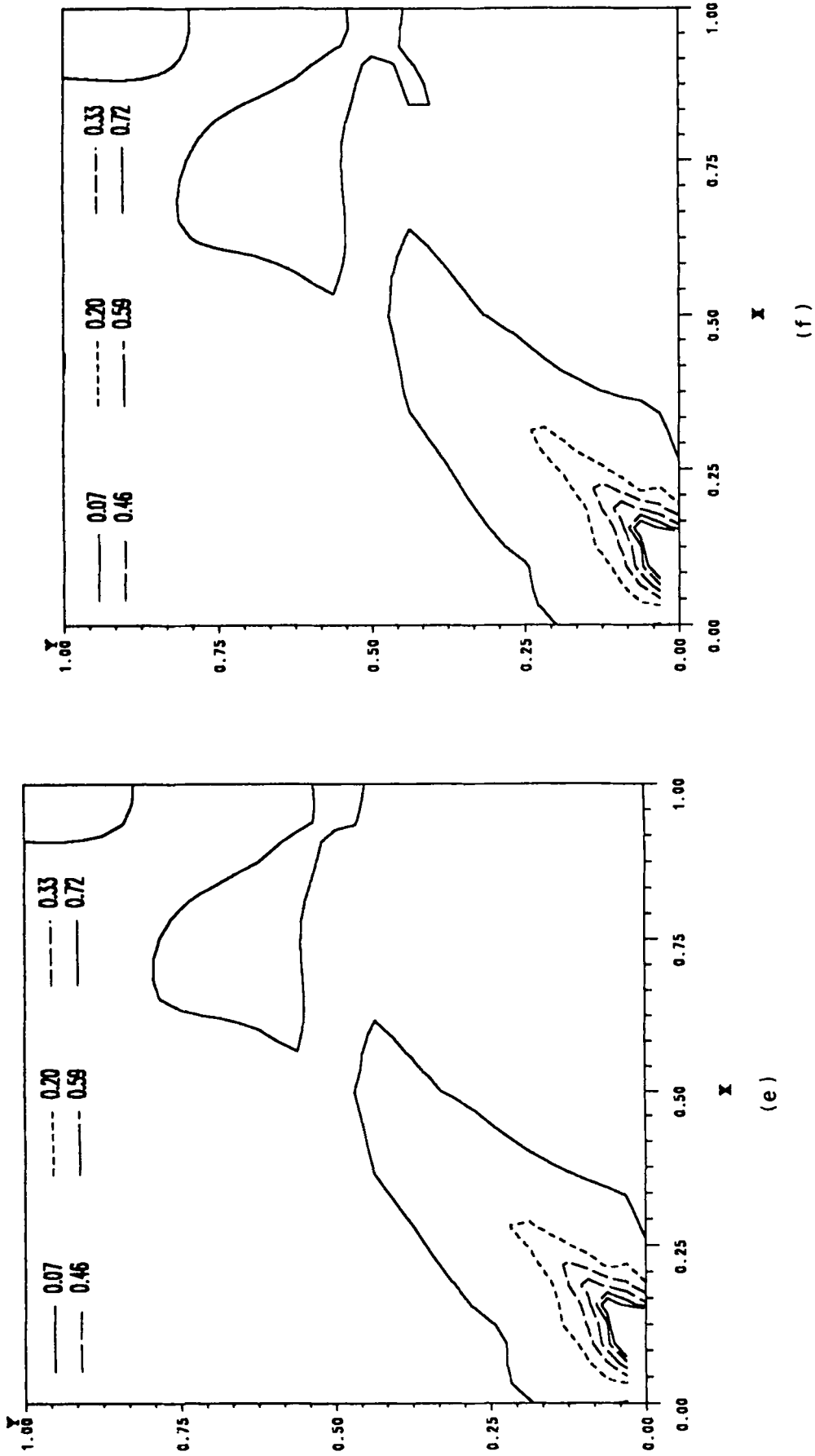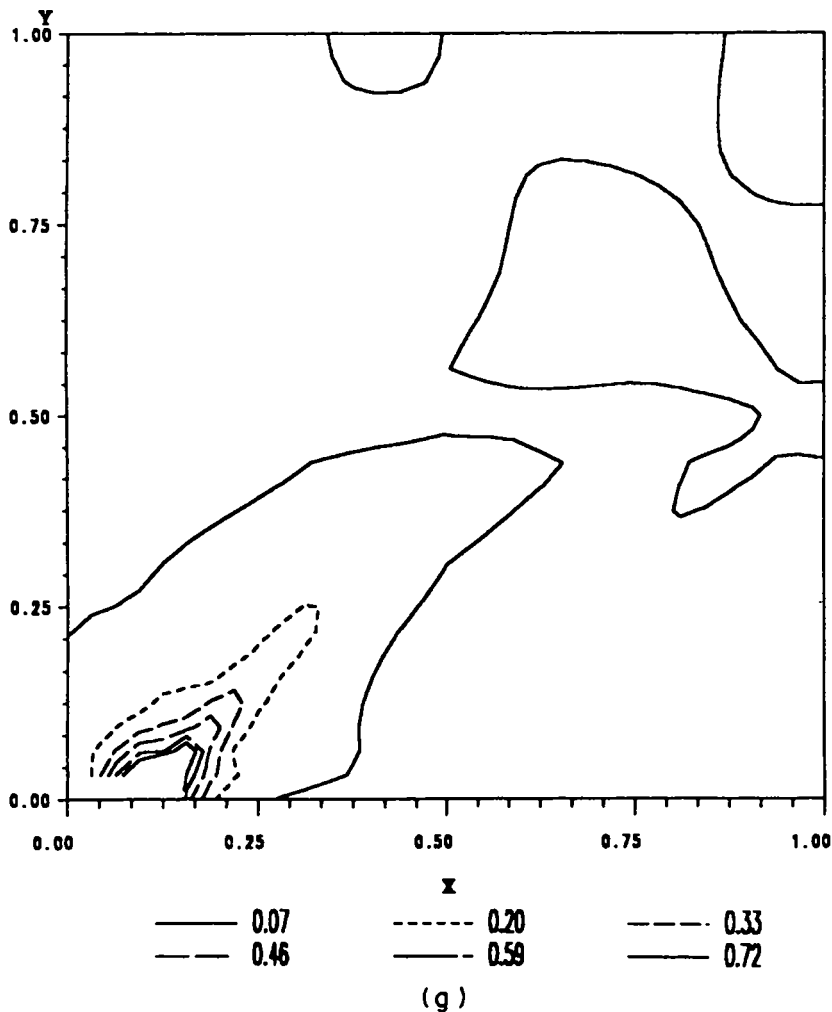
Fig. 10—*continued*.

Fig. 10—continued.

Fig. 10—continued.

Also only the material near the void tip is heated up significantly. At $\gamma_{avg} = 0.0333$, the maximum temperature reached at a point near the void tip equals 157°C. However, if the body were made of a rigid/perfectly plastic material with a flow stress of 333 MPa and deformed homogeneously in simple compression to an average strain of 0.0333, the temperature rise would equal only 2.85°C, assuming that all of the plastic work done has been converted into heat.

Finally, we note that in both cases studied above, contours of distinct values of ε travel at different speeds. The speed of propagation also depends upon the average strain reached in the body.

Even though the deformations could be continued further, they were not mainly because the CPU time required exceeded our allotment and it was felt that the deformations had developed into well-defined shear bands.

4. CONCLUSIONS

We have studied the problem of the initiation and growth of shear bands in plane strain deformations of a thermally softening viscoplastic body containing a void and two symmetrically placed layers made of a viscoplastic material that differs from the matrix material in the value of the flow stress in a quasistatic simple compression test. When the layer material is stronger than the matrix material, a shear band first originates from the void tip. This band propagates into the matrix material at an angle of approximately 45° to the horizontal, the axis of loading being vertical. Two bands also initiate from points

where the layer meets the traction free boundary and these bands propagate into the matrix material along $\pm 45°$ directions. When the void has coalesced, the severely deforming region surrounding the band around the void tip starts receding. Eventually three bands form at an average strain of 0.044 when the maximum principal logarithmic strain and the temperature rise equal 0.134 and 133°C, respectively. However, when the layer material is weaker than the matrix material, bands initiating from the void tip and the layer edges propagate into the matrix and the layer, respectively. The band propagating in the layer bifurcates into two bands that propagate into the matrix material in the direction of maximum shearing stress. One of these bands eventually merges with that initiating from the void tip. The severely deformed region in this case is quite different from the one when the layer material is stronger than the matrix material.

REFERENCES

Anand, L., Kim, K. H. and Shawki, T. G. (1987). Onset of shear localization in viscoplastic solids. *J. Mech. Phys. Solids* **35**, 381–399.

Anand, L., Lush, A. M. and Kim, K. H. (1988). Thermal aspects of shear localization in viscoplastic solids. In *Thermal Aspects in Manufacturing* (Edited by M. H. Attia and L. Kops), Vol. 30, pp. 89–103. ASME, New York.

Bai, Y. L. (1981). A criterion for thermoplastic shear instability. In *Shock Waves and High Strain Rate Phenomenon in Metals* (Edited by M. A. Meyers and L. E. Murr), pp. 277–283. Plenum Press, New York.

Bathe, K. J. (1982). *Finite Element Procedures in Engineering Analysis*. Prentice-Hall, Englewood Cliffs, New Jersey.

Batra, R. C. (1987a). The initiation and growth of, and the interaction among adiabatic shear bands in simple and dipolar materials. *Int. J. Plasticity* **3**, 75–89.

Batra, R. C. (1987b). Effect of material parameters on the initiation and growth of adiabatic shear bands. *Int. J. Solids Structures* **23**, 1435–1446.

Batra, R. C. (1988). Effect of nominal strain-rate on the initiation and growth of adiabatic shear bands. *ASME J. Appl. Mech.* **55**, 229–230.

Batra, R. C. and Liu, D. S. (1989). Adiabatic shear banding in plane strain problems. *ASME J. Appl. Mech.* **56**, 527–534.

Batra, R. C. and Liu, D. S. (1990). Adiabatic shear banding in dynamic plane strain compression of a viscoplastic material. *Int. J. Plasticity* **6**, 231–246.

Batra, R. C. and Zhang, X.-T. (1990). Shear band development in dynamic loading of a viscoplastic cylinder containing two voids. *Acta Mechanica* (in press).

Burns, T. J. (1985). Approximate linear stability analysis of a model of adiabatic shear band formation. *Q. Appl. Math.* **43**, 65–84.

Clifton, R. J. (1980). Adiabatic shear banding. In *Material Response to Ultra High Loading Rates*, Chapter 8, pp. 129–142. NRC National Material Advisory Board, U.S.A., Report No. NMAB-356.

Clifton, R. J., Duffy, J., Hartley, K. A. and Shawki, T. G. (1984). On critical conditions for shear band formation at high strain rates. *Scripta Metallurgica* **18**, 443–448.

Coleman, B. D. and Hodgdon, M. L. (1985). On shear bands in ductile materials. *Archs Ration. Mech. Analysis* **90**, 219–247.

Costin, L. S., Crisman, E. E., Hawley, R. H. and Duffy, J. (1979). On the localization of plastic flow in mild steel tubes under dynamic torsional loading. *Int. Phys. Conf.* Ser. No. **47**, 90–100.

Hartley, K. A., Duffy, J. and Hawley, R. H. (1987). Measurement of the temperature profile during shear band formation in steels deforming at high strain rates. *J. Mech. Phys. Solids* **35**, 283–301.

Hughes, T. J. R. (1987). *The Finite Element Method. Linear Static and Dynamic Finite Element Analysis*. Prentice-Hall, Englewood Cliffs, New Jersey.

Johnson, W. (1987). Henri Tresca as the originator of adiabatic heat lines. *Int. J. Mech. Sci.* **29**, 301–310.

LeMonds, J. and Needleman, A. (1986a). Finite element analyses of shear localization in rate and temperature dependent solids. *Mech. Mater.* **5**, 339–361.

LeMonds, J. and Needleman, A. (1986b). An analysis of shear band development incorporating heat conduction. *Mech. Mater.* **5**, 363–373.

Marchand, A. and Duffy, J. (1988). An experimental study of the formation process of adiabatic shear bands in a structural steel. *J. Mech. Phys. Solids* **36**, 251–283.

Massey, H. F. (1921). The flow of metal during forging. *Proc. Manchester Assoc. Engrs*, pp. 21–26. Reprinted by the National Machinery Co., Tiffon, Ohio (1946).

Merzer, A. M. (1982). Modeling of adiabatic shear band development from small imperfections. *J. Mech. Phys. Solids* **30**, 323–338.

Molinari, A. and Clifton, R. J. (1987). Analytic characterization of shear localization in thermoviscoplastic materials. *ASME J. Appl. Mech.* **54**, 806–812.

Moss, G. L. (1981). Shear strain, strain rate and temperature changes in adiabatic shear band. In *Shock Waves and High Strain Rate Phenomenon in Metals* (Edited by M. A. Meyer and L. E. Murr), pp. 299–312. Plenum Press, New York.

Needleman, A. (1989). Dynamic shear band development in plane strain. *ASME J. Appl. Mech.* **56**, 1–9.

Recht, R. F. (1964). Catastrophic thermoplastic shear. *ASME J. Appl. Mech.* **31**, 189–193.

Staker, M. R. (1981). The relation between adiabatic shear instability strain and material properties. *Acta Met.* **29**, 683–689.

Tresca, H. (1878). On further application of the flow of solids. *Proc. Inst. Mech. Engrs* **30**, 301–345.

Wright, T. W. (1987). Steady shearing in a viscoplastic solid. *J. Mech. Phys. Solids* **35**, 269–282.

Wright, T. W. and Batra, R. C. (1985). The initiation and growth of adiabatic shear bands. *Int. J. Plasticity* **1**, 205–212.

Wright, T. W. and Batra, R. C. (1987). Adiabatic shear bands in simple and dipolar plastic materials. In *Proc. IUTAM Symp. on Macro- and Micro-mechanics of High Velocity Deformation and Fracture* (Edited by K. Kawata and J. Shioiri), pp. 189–201. Springer, New York.

Wright, T. W. and Walter, J. W. (1987). On stress collapse in adiabatic shear bands. *J. Mech. Phys. Solids* **35**, 701–716.

Wu, F. H. and Freund, L. B. (1984). Deformation trapping due to thermoplastic instability in one-dimensional wave propagation. *J. Mech. Phys. Solids* **32**, 119–132.

Zener, C. and Hollomon, J. H. (1944). Effect of strain rate on plastic flow of steel. *J. Appl. Phys.* **14**, 22–32.

Zhu, Z. G. and Batra, R. C. (1990). Dynamic shear band development in plane strain compression of a viscoplastic body containing a rigid inclusion. *Acta Mechanica* **84**, 89–107.